JMEPEG (2012) 21:2680–2683
DOI: 10.1007/s11665-012-0277-1

1059-9495/$19.00

Torsional Properties of TiNi Shape Memory Alloy Tape for Rotary Actuator

K. Takeda, H. Tobushi, K. Mitsui, Y. Nishimura, and K. Miyamoto

(Submitted March 9, 2012; in revised form May 28, 2012)

In order to develop novel shape memory actuators, the torsional deformation of a shape memory alloy (SMA) tape and the actuator models driven by the tape were investigated. The results obtained can be summarized as follows. In the SMA tape subjected to torsion, the martensitic transformation appears along both edges of the tape due to elongation of these elements and grows to the central part. The fatigue life in both the pulsating torsion and alternating torsion is expressed by the unified relationship of the dissipated work in each cycle. Based on an opening and closing door model and a solar-powered active blind model, the two-way rotary driving actuator with a small and simple mechanism can be developed by using torsion of the SMA tape.

Keywords intermetallics, mechanical testing, non-ferrous metals

1. Introduction

One of the main materials which have activated the research on the intelligent materials is shape memory alloy (SMA) (Ref 1, 2). The main characteristics of SMA are the shape memory effect (SME) and superelasticity (SE). Thanks to these characteristics, SMAs are used in the driving elements of actuators, heat engines, robots, and medical instruments. The SME and SE appear as a result of a martensitic transformation (MT). In a recent study using the torsional deformation of a TiNi SMA tube, twist in the blades of rotor aircraft was investigated in order to improve the flight performance (Ref 3, 4). In practical applications making use of SMA tapes, torsional deformation can be obtained simply by gripping both ends without any mechanical process. If the characteristics of SE are exploited, a high performance of energy storage can be achieved similar to that of a torsion bar. In this way of using torsional characteristics of SMA tapes, simple and small actuators can be developed. Therefore, the authors investigated the basic deformation properties of an SMA tape in torsion (Ref 5, 6).

In the present paper, in order to develop the rotary actuators driven by SMA tapes, the torsional deformation properties of TiNi SMA tapes are investigated. The two-way motions of an opening and closing door model and a solar-powered active blind model driven by SMA tapes are demonstrated.

This article is an invited paper selected from presentations at the International Conference on Shape Memory and Superelastic Technologies 2011, held November 6-9, 2011, in Hong Kong, China, and has been expanded from the original presentation.

K. Takeda, H. Tobushi, K. Mitsui, and **Y. Nishimura**, Aichi Institute of Technology, 1247 Yachigusa, Yakusa-cho, Toyota, Aichi 470-0392, Japan; and **K. Miyamoto**, Churyo Engineering Co., Ltd., 60-1 Kutanjo, Iwatsuka-cho, Nakamura-ku, Nagoya 453-0862, Japan. Contact e-mail: q11801qq@aitech.ac.jp.

2. Torsional Deformation Properties of SMA Tape

2.1 Material

The materials used in the experiment were Ti-50.18at%Ni SMA tape with a thickness of $t = 0.25$ mm and a width of $w = 5$ mm. The specimen was a uniform flat tape of length $L = 60$ mm. The gauge length of the specimen was $l = 40$ mm. The transformation temperatures obtained from the DSC test were $M_s = 304$ K (31 °C), $M_f = 266$ K (−7 °C), $A_s = 319$ K (46 °C), and $A_f = 359$ K (86 °C).

2.2 Twisted State

The photographs of the twisted SMA tape are shown in Fig. 1 for each angle of twist. The left side shows the fixed end and the right side the twisted end. The crossover point of the upper and lower surfaces of the SMA tape propagates from the twisting end at the angle of twist per unit length $\theta = 39.3$ rad/m (total angle of twist $\phi = \pi/2$) and reaches the central part of the specimen at $\theta = 78.5$ rad/m ($\phi = \pi$). We note that both edges of the tape are elongated by twisting since both ends are axially fixed. Therefore, tensile stress is induced along both edges, and the stress state becomes different from the simple shear (Ref 7) and much more complex.

2.3 Observation of Martensitic Transformation by Thermography

The temperature distribution on the surface of the SMA tape at each angle of twist during the torsional deformation obtained by the infrared thermography is shown in Fig. 2. In Fig. 2, the upper side in each case shows the twisting part and the lower side shows the fixed part. Maximum temperature T_{max} on the surface of the specimen appears along the edge of the tape, and the exothermic MT occurs in this part and grows toward the central part of the specimen. The temperature rise along the

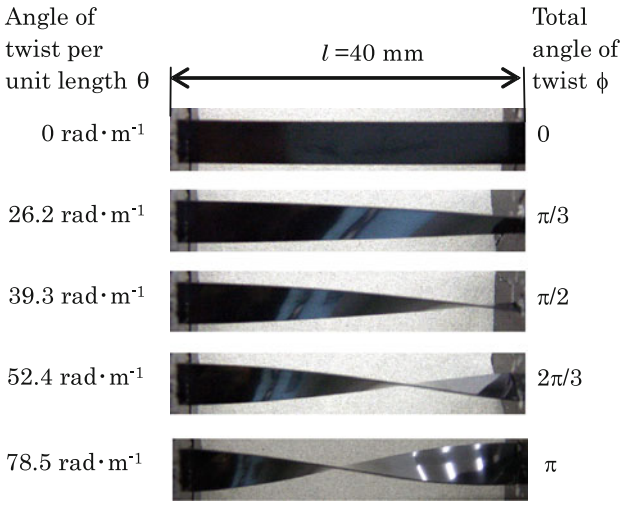

Fig. 1 Photographs of twisted SMA tape at each angle of twist

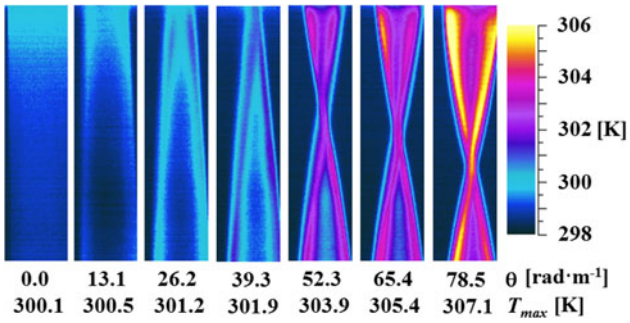

Fig. 2 Thermograms showing temperature distribution on the surface of the SMA tape appeared due to the phase transformation under tortion

edge of the tape starts at the angle of twist per unit length θ = 26.2 rad/m. This angle of twist per unit length corresponds to the tensile strain at the edge of the tape of 0.3% and coincides with the MT starting condition. The maximum temperature of the specimen occurs along the edge of the tape and the high temperature region propagates toward the central part with an increase in angle of twist. Therefore, the MT grows preferentially based on the elongation along the edge of the tape.

2.4 Torsional Deformation

The relationships between torque M and angle of twist per unit length θ obtained by the pulsating torsion test and the alternating torsion test for the maximum angle θ_m = 78.5 rad/m are shown in Fig. 3 and 4, respectively. The variation in angle of twist in the pulsating torsion is 0° (flat) → 180° (twisted) → 0° (flat) in one cycle and that in the alternating torsion is 0° (flat) → 180° (twisted) → 0° (flat) → −180° (twisted in the opposite direction) → 0° (flat) in one cycle. In the case of the pulsating torsion, the curve between M and θ is expressed almost by a straight line in the initial loading process. In the unloading process, the early slope of the curve is steep and thereafter becomes to be the plateau stage. In the reloading process, the early curve is almost parallel to the initial loading curve and thereafter the slope of the curve becomes steep. In the case of the alternating torsion, the twisting in the reverse

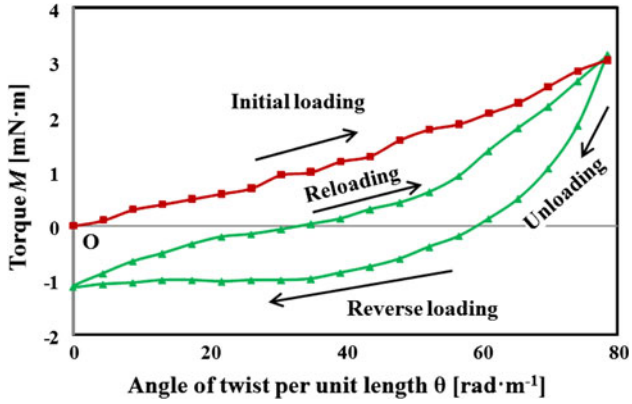

Fig. 3 Relationship between torque M and angle of twist per unit length θ obtained by the pulsating torsion tests for maximum angle θ_m = 78.5 rad/m

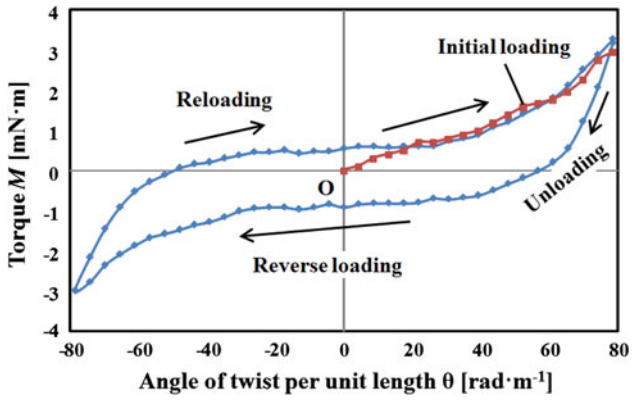

Fig. 4 Relationship between torque M and angle of twist per unit length θ obtained by the alternating torsion tests for maximum angle θ_m = 78.5 rad/m

direction to the initial twisting direction was carried out. The reverse loading and unloading curves are almost similar to the initial loading and unloading curves except for the early stage, closely symmetric with respect to an origin. The point at the end of the reloading curve almost coincides with the point at which the initial unloading started, showing the return-point memory in the pulsating and alternating torsion.

The area surrounded by the hysteresis loop of the torque-angle curve of twist shown in Fig. 3 and 4 expresses the dissipated work per unit length W_d. The value of W_d in the alternating torsion is larger than that in the pulsating torsion by 3.5 times.

2.5 Torsional Fatigue Properties

The torsion fatigue test machine was driven by a motor (Ref 6). The motor was controlled at 600 rpm and therefore the frequency of the fatigue test was 10 Hz. The relations between the maximum angle of twist per unit length θ_m and the number of cycles to failure N_f obtained from the torsion fatigue test are shown in Fig. 5. The number of cycles to failure N_f decreases with an increase in the maximum angle of twist per unit length θ_m. This relation is approximated by a straight line on the logarithmic graph. The fatigue life curve seems therefore to be expressible by the following Eq 1

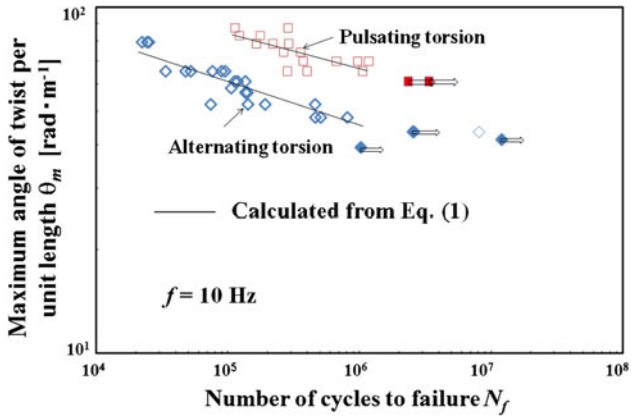

Fig. 5 Relationship between maximum angle of twist per unit length and number of cycles to failure

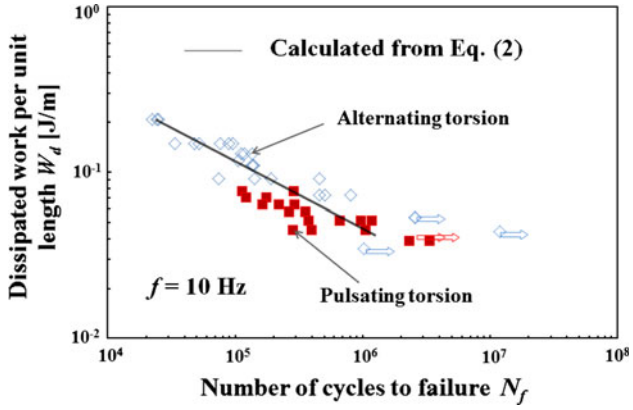

Fig. 6 Relationship between dissipated work per unit length and number of cycles to failure

$$\theta_m \cdot N_f^{\beta} = \alpha, \qquad \text{(Eq 1)}$$

where α and β represent θ_m in $N_f = 1$ and the slope of the log θ_m – log N_f curve, respectively. The calculated results obtained from Eq 1 for $\beta = 0.1$, $\alpha = 265$ rad/m in pulsating torsion and for $\beta = 0.13$, $\alpha = 310$ rad/m in alternating torsion are shown by the solid lines in Fig. 5. As can be seen, the fatigue life curves are well matched by the solid calculation lines. The number of cycles to failure N_f for alternating torsion is smaller than that for pulsating torsion by 1/5.

The relationship between the dissipated work per unit length W_d and the number of cycles to failure N_f is shown in Fig. 6. The relationships for the pulsating torsion and the alternating torsion are located almost on the same line. Both fatigue lives of the pulsating torsion and the alternating torsion are therefore expressed by the unified relationship between N_f and W_d in Eq 2

$$W_d \cdot N_f^{\lambda} = \mu \qquad \text{(Eq 2)}$$

where μ and λ represent W_d at $N_f = 1$ and the slope of the log W_d – log N_f curve, respectively. The calculated result by Eq 2 for $\lambda = 0.382$ and $\mu = 9$ J/m is shown by the solid line in Fig. 6. As can be seen, the overall inclinations are approximated by the solid line. The dissipated work corresponding to the fatigue limit may exist at 0.04-0.05 J/m.

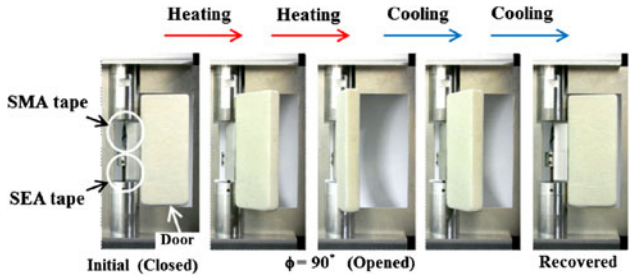

Fig. 7 Photographs of two-way rotary movement of a door driven by SMA tape and SEA tape during heating and cooling

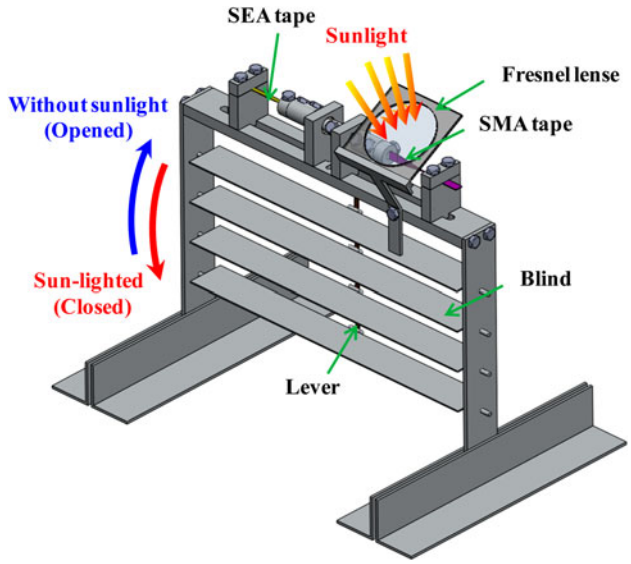

Fig. 8 Structure of the solar-powered active blind model driven by twisting of SMA tape and SEA tape

3. Rotary Actuators Driven by SMA Tape

3.1 Two-Way Opening and Closing Door Model

Photographs of the rotary movement of an opening and closing door model using an SMA tape which shows the SME and a superelasticity alloy (SEA) tape which shows the SE at room temperature (RT) are shown in Fig. 7. The SMA tape is the same as the specimen used in the torsion test. The SEA tape with a thickness of $t = 0.25$ mm and a width of $w = 2.5$ mm was a TiNi SEA tape which was heat-treated to memorize a flat plane. In the initial state at RT, the SEA tape was mounted to be in a flat plane and the SMA tape was mounted at the total angle of twist $\phi = \pi/2$. The SMA tape was heated by joule heat through electric current. As can be seen in Fig. 7, the door is closed in the initial state, since torque of SEA tape M_{SEA} is larger than that of the SMA tape M_{SMA}. Since recovery torque appears by heating the SMA tape and the relation of the torque changes into $M_{SMA} > M_{SEA}$, the SMA tape recovers a flat plane and therefore the door is opened. When the SMA tape is cooled thereafter, the relation of torque varies again into $M_{SMA} < M_{SEA}$. Therefore, the SEA tape recovers a flat plane, resulting in closing the door. Thus, if two kinds of SMA tapes which show the SME and SE are used, a two-way rotary

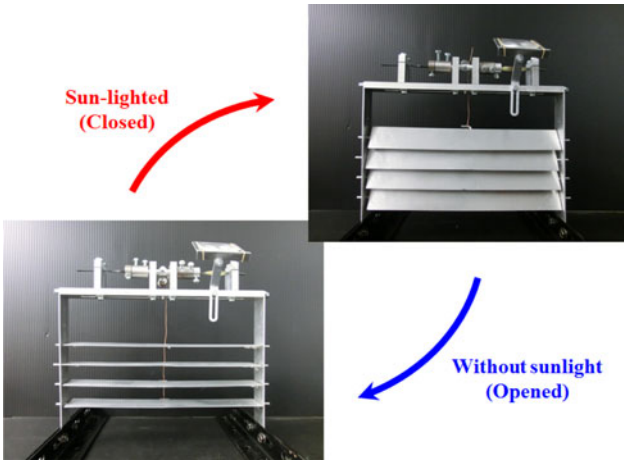

Fig. 9 Photographs of two-way motion of the solar-powered active blind model

driving element with a small and simple mechanism can be developed.

3.2 Solar-Powered Active Blind Model

The structure and the photographs of two-way motion of the solar-powered active blind model are shown in Fig. 8 and 9, respectively. Both the SMA tape and the SEA tape were the same as those used in the door model. In the initial state, the SEA tape was mounted to be in a flat plane and the SMA tape was mounted at the total angle of twist $\phi = \pi/2$. The SMA tape was heated by sunlight through a Fresnel lens. Since recovery torque appears in SMA tape by heating the tape, the blind is closed through a crank and a lever. When the sunlight is shut out, the SMA tape is cooled and the SEA tape recovers a flat plane, resulting in opening the blind. The fatigue life of the SMA tape in the proposed models must be close to the fatigue life obtained by the pulsating fatigue test which is longer than 3×10^6 cycles at the maximum angle of twist $\phi_m = \pi/2$ with the maximum angle of twist per unit length $\theta_m = 39.3$ rad/m. Therefore, if the proposed models are twisted 100 times a day, the service life will be longer than 50 years.

4. Conclusions

In order to develop the rotary driving element with SMA tapes, the torsional deformation properties of a TiNi SMA tape and actuator models driven by SMA tapes were investigated. The results obtained can be summarized as follows.

(1) In the SMA tape subjected to torsion, the MT appears along the edge of the tape due to elongation of this part and grows to the central part. The dissipated work per unit length in the alternating torsion is larger than that in the pulsating torsion.
(2) The fatigue life in the alternating torsion is shorter than that in the pulsating torsion. The fatigue life in both the pulsating and alternating torsions is expressed by a unified power function of the dissipated work in each cycle.
(3) Based on the two-way motion of an opening and closing door model and a solar-powered active blind model driven by two kinds of SMA tape, it is confirmed that the two-way rotary driving actuator with a small and simple mechanism can be developed by using torsion of the SMA tapes.

References

1. S. Miyazaki, Ed., *Shape Memory and Superelastic Technologies—2007*, ASM international, Materials Park, OH, 2008
2. K. Otsuka and C.M. Wayman, *Shape Memory Materials*, Cambridge University Press, Cambridge, 1998
3. J.H. Mabe, F.T. Calkins, and R.T. Ruggeri, Full-Scale Flight Tests of Aircraft Morphing Structures Using SMA Actuators, *Proc. SPIE*, 2007, **6525/65251C**, p 1–12
4. J.H. Mabe, R.T. Ruggeri, E. Rosenzweig, and C.J. Yu, Nitinol Performance Characterization and Rotary Actuator Design, *Proc. SPIE*, 2004, **5388**, p 95–109
5. H. Tobushi, T. Sakuragi, and Y. Sugimoto, Deformation and Rotary Driving Characteristics of a Shape-Memory Alloy Thin Strip Element, *Mater. Trans.*, 2008, **49**, p 151–157
6. H. Tobushi, E.A. Pieczyska, W.K. Nowacki, T. Sakuragi, and Y. Sugimoto, Torsional Deformation and Rotary Driving Characteristics of SMA Thin Strip, *Arch. Mech.*, 2009, **61**, p 241–257
7. E.A. Pieczyska, S.P. Gadaj, J. Luckner, W.K. Nowacki, and H. Tobushi, Martensite and Reverse Transformation during Complete Cycle of Simple Shear of NiTi Shape Memory Alloy, *Strain*, 2009, **45**, p 93–100